Network of epicenters of the Olami-Feder-Christensen model of earthquakes

Tiago P. Peixoto* and Carmen P. C. Prado†
Instituto de Física, Universidade de São Paulo, Caixa Postal 66318, 05315-970 São Paulo, São Paulo, Brazil
(Received 25 February 2006; published 31 July 2006)

We study the dynamics of the Olami-Feder-Christensen (OFC) model of earthquakes, focusing on the behavior of sequences of epicenters regarded as a growing complex network. Besides making a detailed and quantitative study of the effects of the borders (the occurrence of epicenters is dominated by a strong border effect which does not scale with system size), we examine the degree distribution and the degree correlation of the graph. We detect sharp differences between the conservative and nonconservative regimes of the model. Removing border effects, the conservative regime exhibits a Poisson-like degree statistics and is uncorrelated, while the nonconservative has a broad power-law-like distribution of degrees (if the smallest events are ignored), which reproduces the observed behavior of real earthquakes. In this regime the graph has also an unusually strong degree correlation among the vertices with higher degree, which is the result of the existence of temporary attractors for the dynamics: as the system evolves, the epicenters concentrate increasingly on fewer sites, exhibiting strong synchronization, but eventually spread again over the lattice after a series of sufficiently large earthquakes. We propose an analytical description of the dynamics of this growing network, considering a Markov process network with hidden variables, which is able to account for the mentioned properties.

DOI: 10.1103/PhysRevE.74.016126 PACS number(s): 05.65.+b, 89.75.Da, 89.75.Kd, 45.70.Ht

I. INTRODUCTION

Several different phenomena in nature spontaneously exhibit scale-invariant statistics. An attempt to identify a supposed basic mechanism behind this behavior was made by Bak *et al.* [1], who introduced the concept of self-organized criticality (SOC). SOC is characterized by slowly driven systems, with fast avalanchelike bursts of dissipation. Despite probably not being the sole explanation for scale invariance in nature, a wide range of systems do appear to exhibit SOC, such as sandpiles [1], forest fires [2], and earthquakes [3]. However, no general framework for SOC systems exists, and the mechanism behind it is not very well understood. In particular, the existence of SOC in nonconservative systems is still debated [4–6]. This discussion is frequently focused on one of the most studied and archetypal nonconservative SOC models, the Olami-Feder-Christensen (OFC) model for earthquakes. Despite being defined by very simple rules (see Sec. II), this model possesses very rich dynamics, and is able to reproduce a wide range of statistics of real earthquakes, such as the Gutenberg-Richter law for the distribution of event sizes [3,7] and the Omori law for fore- and aftershocks [8,9].

In this work we concentrate on the behavior of the epicenters in the OFC model, in both the conservative and nonconservative regimes, studied as a growing complex network with scale-free behavior [10,11].

As known previously [4,12], we confirm that in both regimes epicenters are more frequent closer to the border, and we study this effect in detail. We show, however, that this border effect does not scale with system size, and should not therefore be considered representative of the dynamics of the model in the thermodynamic limit. The length of the effect is dependent on the level of dissipation, and is relatively large for the range of parameters normally studied, especially when close to the conservative limit, where an exponentially decaying layer dominates, and it is hard to observe anything else other than this border effect. The existence of this nonscaling border is in accordance with what was found in [4], that only earthquakes from a smaller internal subset of the lattice exhibit finite-size scaling in the event size statistics.

We turn then to the dynamics of epicenters. Recently there has been an increasing interest in complex networks [13] as a tool for describing very diverse systems, many of which exhibit a type of scale invariance that seems to be due to a general mechanism of preferential attachment [14,15]. In order to study the epicenter dynamics in the OFC model, we construct a network of consecutive epicenters in the bulk, and examine its properties in more detail.[1]

The network of epicenters, in the nonconservative regime, shows scale invariance in the degree statistics, if the epicenters of the smaller events are discarded. This network has also an unusual correlation among vertices of high degree, which makes it very distinct from networks created with a preferential attachment rule. These results reproduce what has been found by Abe and Suzuki [16,17] for real earthquakes, further contributing to the success of this simple model in capturing the essential earthquake dynamics. We show that this degree correlation seems to be due to the existence of temporary attractors for the dynamics, which shows periods of strong synchronization. We also noticed that a drop in the average in-degree of the network seems to precede big earthquakes, which could in principle be used to predict at least an increase in the probability of big events in a given fault.

*Electronic address: tpeixoto@if.usp.br
†Electronic address: prado@if.usp.br

[1] In a previous study [10], we also analyzed some aspects of the same network, but did not take into account the border effect, and looked only at smaller lattices.

 ©2006 The American Physical Society

We also show that is possible to reproduce some of the characteristics of the complex epicenter network found in the nonconservative version of the OFC model by defining a growing procedure based on a Markov chain with hidden variables. To each possible epicenter (vertex) is attached a hidden variable, and the probability of connections among epicenters (related to the time sequence of events) is now given as a function of the hidden variable of both vertices (instead of a simple preferential attachment rule, as in a Barabási-Albert-type network [15]).

This paper is organized as follows. In Sec. II we briefly present the Olami-Feder-Christensen model for earthquakes; in Sec. III we discuss in detail the way the spatial distribution of epicenters depends on the distance to the borders, in the conservative, nonconservative, and "almost conservative" regimes; in Sec. IV we review the way we can build a scale-free network from the time series of epicenters, and present the main properties of this network when the border effect is discarded. This network, although showing a scale-free behavior, is quite different from Barabási-Albert-type networks, with a strong correlation among vertices with high degree. In Sec. V we show how we can grow a network with similar properties based on a Markov chain process with hidden variables and, finally, in Sec. VI, we summarize our results.

II. THE OFC MODEL

The OFC model [3] was inspired by the Burridge-Knopoff spring-block model [18], and is defined as a two-dimensional (2D) coupled map on a square lattice. To each site (i,j) in the lattice is assigned a "tension" z_{ij}, initially chosen at random from the interval $[0,z_c[$. The entire system is driven slowly, with every z_{ij} increasing uniformly. Whenever a site reaches the threshold tension ($z_{ij}=z_c$), an avalanche starts (the "earthquake"). The first site to reach z_c and start an avalanche is called the epicenter. A fraction α of the tension of the toppling site is transferred to each of its four neighbors ($z_{i\pm1,j\pm1}=z_{i\pm1,j\pm1}+\alpha z_{ij}$), and its tension is set to zero ($z_{ij}=0$). If any of the neighbors acquires a tension $z_{i\pm1,j\pm1}\geqslant z_c$, the same toppling rules are applied, until there are no more sites in the system with $z_{ij}\geqslant z_c$. Without loss of generality, we set $z_c=1$. The total number of sites that topple until the avalanche is over is called the "size" of the avalanche. The parameter α defines the level of local conservation of the system. For $\alpha=0.25$ the system is locally conservative and for $\alpha<0.25$ it is dissipative. We consider here only the case with open boundary conditions, i.e., the sites at the border of the lattice transfer tension to nonexisting neighbors, so the system is always globally nonconservative, but tends to conservative in the thermodynamic limit if $\alpha=0.25$.

III. INFLUENCE OF THE BORDERS ON THE FREQUENCY OF EPICENTERS

We find that, in the stationary regime of the OFC model, the number of times a site is an epicenter varies according to how close that site is to the border, with epicenters closer to the border occurring much more often. We will refer to this excess of epicenters in the borders as the *border effect*. Figure 1 shows the average frequency with which a site was an epicenter, given its distance from the border, for $\alpha=0.25$, 0.249, 0.22, and 0.18. We have gathered statistics from two lattice sizes $L=400$ and 800, and considered at least 6×10^6 events (after the transient). We have considered epicenters only of earthquakes larger than 1 ($s\geqslant2$), since size-1 earthquakes seem to obey their own statistics [19]. We have also considered epicenters that gave rise to larger earthquakes ($s\geqslant30$), to observe the dependence of the border effect on earthquake size.[2]

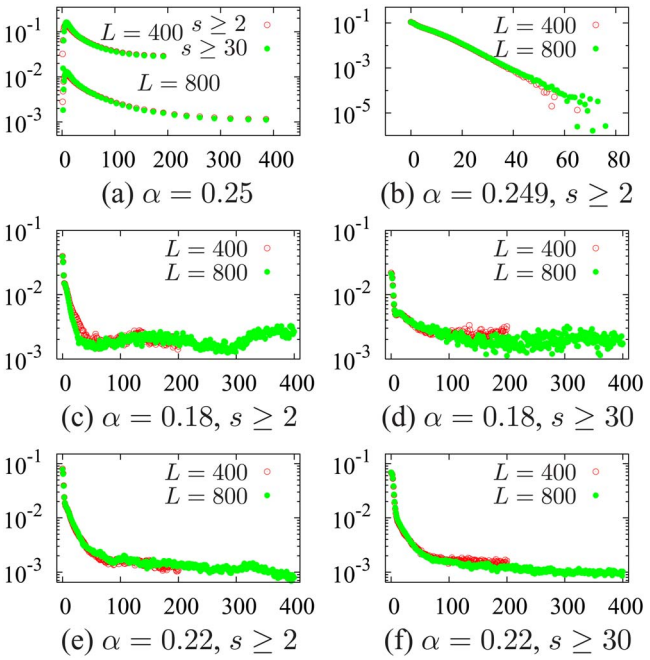

FIG. 1. (Color online) Frequency of epicenters (y axis) as a function of the distance from the border (x axis), for different values of α, L, and earthquakes size s. The data for $L=400$ in (a) were shifted upward for clarity. From (c) to (f) the data for different values of L were collapsed on top of each other by hand. All quantities are dimensionless.

For the conservative regime, as can be seen in Fig. 1(a), the border effect is clearly weaker than in the nonconservative regime, and the decay proceeds slowly toward the bulk. It does not seem to scale with system size. Moreover, the dependence on earthquake size appears to be weak for most of the border effect, except for the very first few layers of sites close to the border.

Figures 1(c)–1(f) also show the same results for the nonconservative case, for $\alpha=0.18$ and 0.22. We notice that the border effect is composed roughly of three parts. First there is a thin region, comprised of the first few sites closest to the border, where the effect is strong and seems to decay exponentially. This region is followed by a thicker layer of sites,

[2]We realize, however, that this is rather coarse, since, due to the power-law distribution of event sizes, there is no characteristic event size to compare to. We wanted only to detect eventual differences in the statistics from the "very small" events. It would also take a much longer time to consider only larger earthquakes.

with a slower but also exponentially decaying effect; and finally there is a third region in which the decay is not exponential and proceeds still more slowly toward the bulk of the system. None of those regions seem to scale with system size, with the possible exception of the third, longer layer. The overall border effect seems, however, to depend on the earthquake size (in the contrast with what was observed in the conservative case), as can be seen in Figs. 1(d) and 1(f), which shows clearly that the border effect decays more slowly toward the bulk of the system if only larger events are considered. In Figs. 1(c)–1(f), the data for lattices of different size L were collapsed by hand, that is, curves were shifted up and down in order to coincide, since statistics are different in each case. The slope and the size of the layers, however, were not changed.

The border effect also depends on α. The closer the system is to the conservative regime, the stronger and thicker is the layer of sites affected by it. Note that for $\alpha=0.249$, the almost conservative case [see Fig. 1(b)], the border effect is so strong that almost no epicenters happen in the bulk of the system, and only the fast exponentially decaying border effect is seen. This indicates that the lattice size $L=800$ is still too small to study the system in this regime. If we compare this figure with Fig. 1(a), we note that there is also evidence of a sharp transition from the nonconservative to the conservative regime of the model, for which the border dependence of epicenters is radically different.

The crucial role of the border in this model was already pointed out by Middleton and Tang [4], who argued that the inhomogeneity introduced by the open boundary inhibits the synchronization of the bulk, which would otherwise reach a periodic state, as happens with a system with periodic boundaries. The resulting "self-organization" would begin at the border and then proceed toward the bulk, following a power law in time. Also, it has been shown in [4] that, while the statistics of event sizes in the OFC model does not seem to obey finite-size scaling (FSS), this behavior is recovered only when events inside a smaller internal subset of the tension lattice are considered. Thus, the existence of nonscaling border effects is to be expected.

We proceed to examine the dynamics of the epicenters in the model, but only those unrelated to the nonscaling border effect. Therefore, unless otherwise noted, we ignored all the epicenters belonging to an outer layer of 100 sites in the lattice, for all the systems studied.

IV. SEQUENCES OF EPICENTERS AS A COMPLEX NETWORK

A graph (or network) is a set of discrete items, called vertices or nodes, with connections between them, called edges or links. An edge connecting vertices i and j is *directed* if it is defined in only one direction (connects vertex i with vertex j, for instance, but not site j with site i) and a graph is said to be directed if its edges are directed. There may be more than one edge between a pair of vertices, and the graph is called in this case a *multigraph*. The number of edges connected to a vertex is called the *degree* of the vertex; since there may be more than one edge between two vertices,

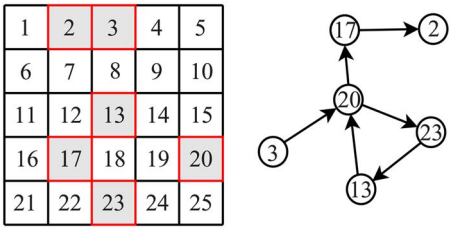

FIG. 2. (Color online) An example of an epicenter graph (right), generated from a sequence of epicenters [marked in red (gray)] from a 5×5 tension lattice (left). The graph corresponds to the following sequence of epicenters: 3, 20, 23, 13, 20, 17, 2.

the degree of a vertex is not necessarily equal to the number of its neighbors. If the graph is directed, it is then possible to talk about *out-degree* (number of edges leaving a vertex) and *in-degree* (number of edges incident to a vertex). The degree distribution of a graph, $P(k)$, gives the probability that a randomly sampled vertex has degree k. Graphs have been the subject of systematic study by mathematicians for some time, but recent years witnessed a growth in the interest in this subject among physicists, with emphasis on large-scale statistical properties of graphs. Many statistical mechanics concepts and techniques have been widely used, and a good review on recent developments in this subject can be found in [13]. We will show that some tools of network theory can help to get a deeper understanding of the dynamics of the OFC model and maybe of the dynamics of real earthquakes.

The sequence of epicenters in the OFC model can be used to construct a directed multigraph in the following manner. Each site that is an epicenter represents a vertex. Two consecutive epicenters are connected by a directed edge, from the first to occur to the second (see Fig. 2). Since, in principle, the same site can become an epicenter two times consecutively, loops are allowed (but do not occur often). It is also possible for the same sequence of epicenters to happen more than once, so parallel edges are also allowed. This graph has certain regularities. The out-degree of every vertex is always equal to the in-degree, except for the very first and last epicenters of the sequence, and therefore the total degree is always an even number. Also, if the direction of the edges is ignored, the graph is always composed of only one component.

We have constructed graphs for the epicenters of the OFC model with $L=400$ and 800, and for $\alpha=0.25$, 0.22, and 0.18. We also considered the graphs for epicenters of different earthquake sizes. We then observed the degree distribution and the degree correlation of the graph. The results for the nonconservative regime are averages over 5–11 graphs, depending on the size of earthquakes considered, each graph with 6×10^6 edges.

A. Degree distribution

Since the in-degree of the network is equal to the out-degree, it is sufficient to describe only one of the two, and here we choose arbitrarily the in-degree.

For the conservative regime [Fig. 3(a)], the in-degree distribution seems to be Poissonian (which gets stretched if

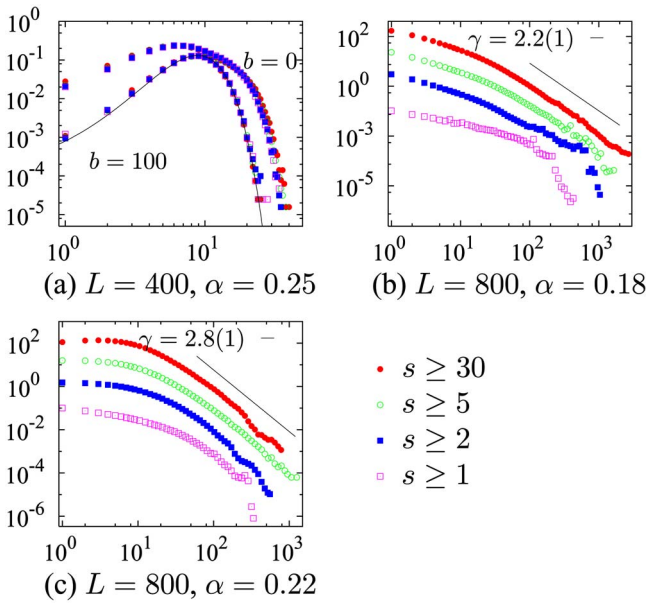

FIG. 3. (Color online) In-degree distribution $P(k)$ (y axis) as a function of the in-degree k (x axis), for different values of L, α, and earthquake size s. In (a) are shown the distributions for two different sizes of the discarded border b, and the solid line is the corresponding Poisson distribution. The data for $b=0$ were shifted upward for clarity. In (b) and (c) the solid line is the result of fitting a power law $k^{-\gamma}$ to the data when $s \geqslant 30$. The data for different earthquake sizes were shifted upward for clarity. All quantities are dimensionless.

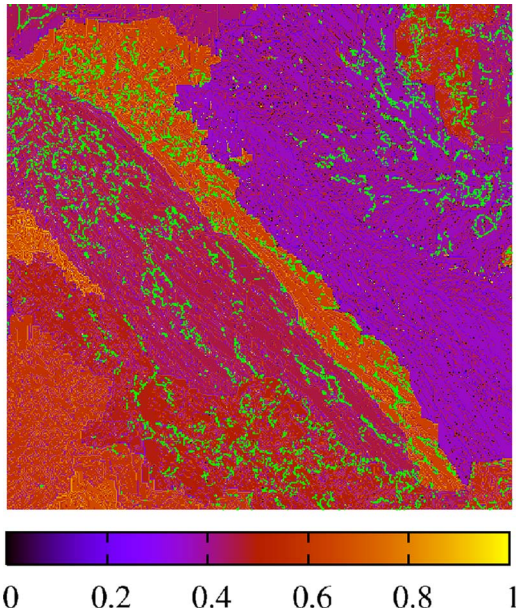

FIG. 4. (Color online) Snapshot of the tension lattice at the stationary state, for $L=800$ and $\alpha=0.18$. The next 10^4 epicenters, for earthquake sizes $s \geqslant 2$, after this configuration, are marked in green (light gray). All quantities are dimensionless.

more sites from the border are considered), indicating that, in this regime, epicenters in the bulk of the lattice occur randomly. Moreover, the degree distribution does not depend on the minimum size of the earthquakes considered.

For the nonconservative regime the situation changes. As can be seen in Figs. 3(b) and 3(c), if only larger earthquakes are considered, the in-degree distribution resembles more a power law. The exponent of the power law seem to be dependent on α, with smaller α leading to steeper lines. For $\alpha=0.22$ and $s \geqslant 30$, in Fig. 3(c), the high fluctuations at the tail of the in-degree distribution represent a lack of statistics, due to an average over only five realizations of the graph, while for $s \geqslant 5$, for instance, the average was over ten different graphs. For both $\alpha=0.22$ and 0.18, the difference of inclination of the power-law region of the distributions is very small between the data for $s \geqslant 5$ and $s \geqslant 30$, indicating that it is not strongly dependent on the lower bound of the considered earthquake sizes, provided it is large enough for the power law to emerge.

B. Correlations between degree distribution and tension distribution in the lattice

It is interesting to observe where the epicenters happen in the tension lattice. As has already been shown in [20], the stationary state of the OFC model, for $\alpha < 0.25$ (nonconservative), exhibits patchy synchronized regions within the bulk of the system with sites that have similar tension, and behaves similarly to the OFC model with periodic boundary conditions, exhibiting heavy synchronization. As can be seen in Fig. 4, for $\alpha=0.18$, the epicenters seem to happen mostly in the frontiers among those synchronized regions, and in valleylike structures inside the plateaus. As only larger earthquakes are considered, the epicenters happen increasingly in smaller and less structured regions (not shown). The same behavior was also observed for $\alpha=0.22$.

In Fig. 5 can be seen the in-degree of a vertex placed in the tension lattice, i.e., the number of times a site was an epicenter, for $\alpha=0.18$ and $s \geqslant 2$. The epicenters seem to be

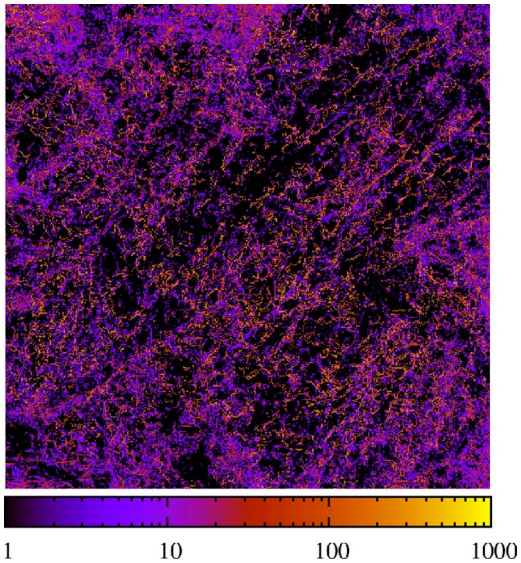

FIG. 5. (Color online) In-degree of vertices placed in the bulk of tension lattice, i.e., the number of times a site was an epicenter, for $L=800$ and $\alpha=0.18$. Only earthquakes with sizes $s \geqslant 2$ were considered. All quantities are dimensionless.

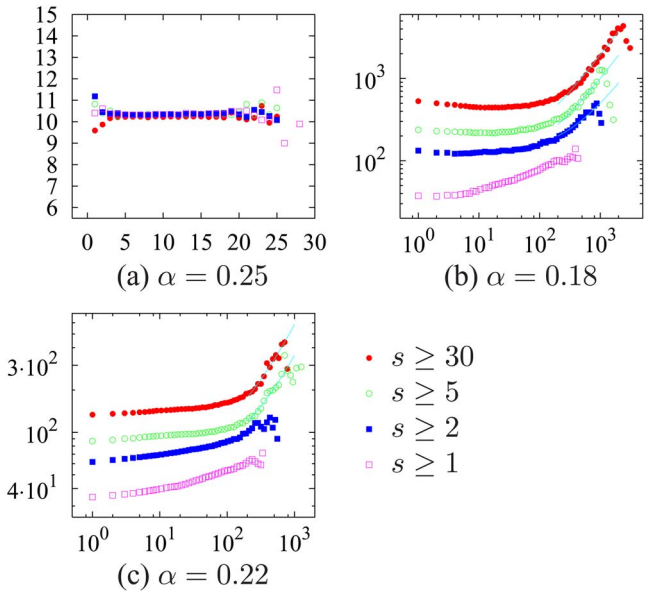

FIG. 6. (Color online) Average in-degree of nearest out-neighbors $k_{NN}(k)$ (y axis) as a function of the in-degree k (x axis), for different values of L, α, and earthquake size s. The solid lines are fitted straight lines. All quantities are dimensionless.

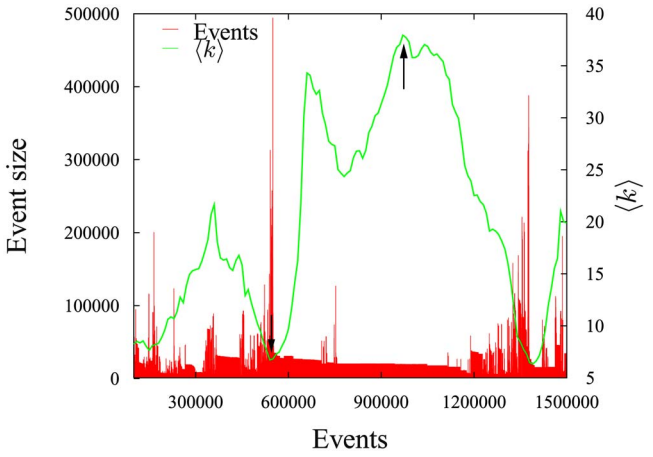

FIG. 7. (Color online) Average in-degree of the subgraph composed only of the last 10^5 events, and the amplitudes of the events that generated the graph. The regions indicated by the arrows correspond to the subgraphs in Figs. 8 and 9. All quantities are dimensionless.

well distributed inside the bulk, but aggregated in stripelike structures. For $s \geqslant 30$ the epicenters seem considerably less aggregated (not shown). For $\alpha = 0.22$ the results were observed to be very similar.

C. Degree correlation

One further basic aspect of the epicenter network which we analyzed was the degree correlation, i.e., how vertices are connected to each other based on their degrees. We look at the average in-degree of the nearest "out-neighbors" of a vertex (vertices that receive an edge coming from it), as a function of the degree of the vertex.

We found that for the conservative regime [Fig. 6(a)], the graph seems to be uncorrelated, with the in-degree of the nearest neighbors being independent on the in-degree of the originating vertex. Together with the in-degree distribution (Poissononian), this puts this graph closer to the class of totally random graphs such as the Erdős-Rényi graph [21].

The situation is again very different for the nonconservative regime [Figs. 6(b) and 6(c)]. In that case, the degrees seem highly correlated, with vertices with high in-degree connecting predominantly to other vertices of high in-degree, which makes the network assortative. The correlation seems to be linear for higher degrees, when only larger earthquakes are considered.[3] Citation networks [14,15] and other networks that are grown with a preferential attachment rule have a quite different behavior, with an in-degree distribution following a power law, but in those cases the degree correlation also decays with a power law [22], converging to a constant value for large in-degrees. Thus, the dynamics responsible for generating this network must be fundamentally different from the dynamics generated by a preferential attachment rule. Recently it has also been found that a very similar network, when constructed with real earthquake data, is also assortative and exhibits similar degree correlations [17].

What indeed is unveiled by this high correlation among high in-degree vertices is an attracting dynamics: Connections from vertices of one type are much more probable to vertices of the same type, eventually trapping the sequence of epicenters in a smaller region of the lattice, stretching the in-degree distribution, and generating the observed in-degree correlation. This trapping seems to be strongly correlated to the occurrence of very large earthquakes, and the large-scale redistribution of tensions that is caused by them. This can be seen in Fig. 7, where is shown the average in-degree of the subgraph composed only of the last 10^5 events, together with the amplitude of the corresponding events. Whenever a large earthquake occurs, the average in-degree drops, meaning that the last epicenters happened in a larger number of sites. In fact the decay of the average in-degree starts before the main big earthquake, and seems to occur together with the smaller events that lead up to it, the so-called foreshocks [8,9,23]. Thus, the large events, together with their foreshocks, are responsible for breaking the attractor, and spreading the epicenters to a larger region. After the sequence of large events, the trapping of epicenters starts again, until the next sequence of large events sweeps it again. Although we did not make an extensive analysis to define the degree of certitude of this observation, monitoring the in-degree of this network may represent a promising way of predicting an increase in the probability of observing large earthquakes in a given fault, and to identify, among the small events, the signature

[3]The in-degree correlation of the graph for $s \geqslant 1$ is also an increasing function, and perhaps also linear. But the lack of vertices of high degree makes it difficult to be certain.

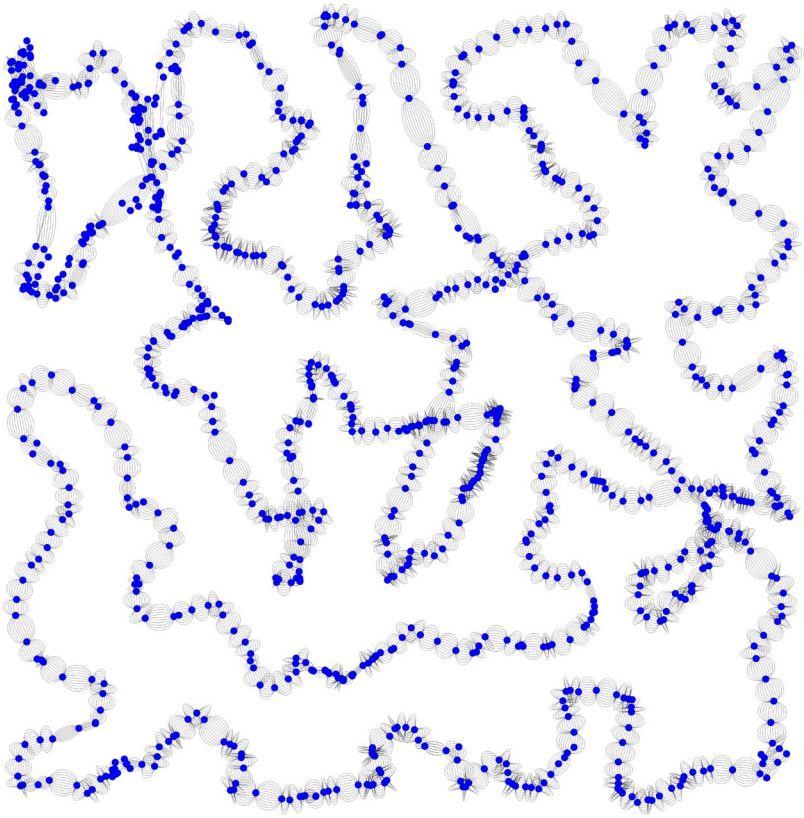

FIG. 8. (Color online) Subgraph composed of 10^4 consecutive epicenters, corresponding to the marked region at the right in Fig. 7.

of the foreshocks that precede a main shock.[4] Since the network of epicenters generated by the OFC model seems to reproduce many aspects of the network of epicenters built from real data [16,17], including the degree correlation mentioned above, it would be interesting to see in more detail if both graphs are actually generated by the same overall dynamics. This, however, would require a more systematic and thorough analysis of real earthquake data, and therefore would be better suited for a separate work.

To illustrate the topology of the graph during both situations, we show a subgraph of the whole network, corresponding to a region of 10^4 events collected during the period that the dynamics is trapped in an attractor (Fig. 8), and just after a large earthquake (Fig. 9), as indicated in Fig. 7. As can be seen in Fig. 8, the attractor region is dominated by synchronization, where the same sequence of $\sim 10^3$ epicenters occurs repeatedly. During the occurrence of the large events, the same subgraph looks like Fig. 9, where synchronization is still present, but in a much smaller degree.

V. MARKOV NETWORKS WITH HIDDEN VARIABLES

In this section we describe a general random graph model, based on hidden variables and a Markov chain. It is based on a similar class of networks developed by Boguñá *et al.* [24], but modified in order to account for the topology of the epicenter graph observed in the OFC model. Our goal is to better understand the type of dynamics that is able to generate graphs with properties examined in the previous section.

Consider a set of N vertices, where $N \gg 1$. To each vertex ν is assigned a hidden variable h_ν, sampled from a distribution $\rho(h)$. A directed multigraph can be constructed via a Markov chain, in the following manner. Starting from a random vertex μ, a directed edge is added from μ to ν with probability $P(\mu \to \nu) \equiv r(h_\mu, h_\nu)$, and likewise from ν to any other vertex ω with probability given by $r(h_\nu, h_\omega)$, and so forth. After a transient stage, the graph will have properties that are entirely defined by $\rho(h)$ and $r(h,h')$. This graph is rather general, and, in fact, every Markov process generates such a graph if the discrete states of the chain are thought of as vertices and the transition as directed edges. With this basic procedure in mind we can proceed to calculate the statistical properties of the graph.

In-degree distribution

As in the network of epicenters, every vertex of the network generated in the way described above has the in-degree equal to the out-degree. Thus, it is sufficient to describe only one of the two. To find the in-degree distribution of this graph, one must consider an ensemble of graphs and the probability in the ensemble of one vertex ν receiving one connection after a time T, $w_\nu(T)$, which is given by

[4]It is important to note that the data in Fig. 7 show only earthquakes that did not initiate inside the discarded outer layer and whose magnitudes tend to be large, and thus are potentially related to the anticipated decay of the average in-degree before a main large event.

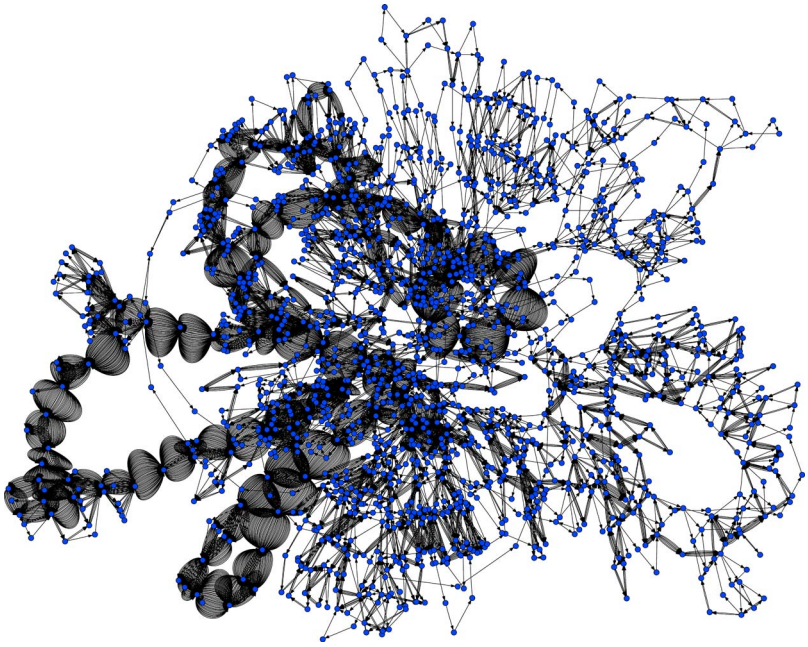

FIG. 9. (Color online) Subgraph composed of 10^4 consecutive epicenters, corresponding to the marked region at the left in Fig. 7.

$$w_\nu(T+1) = \sum_\mu P(\mu \to \nu) w_\mu(T). \tag{1}$$

After a long time T, the system reaches the stationary state $w(\infty)$ given by

$$w(\infty) = \mathbf{P}^n w(\infty), \tag{2}$$

where $\mathbf{P}$ is the transition matrix defined by $P(\mu \to \nu)$, $w(T)$ is the state vector at time T, and n is the period of the solution (we will consider only $n=1$ from now on).

The probability that a vertex μ has in-degree k after a time $T \gg 1$, $P(k|\mu,T)$, is given simply by the binomial distribution,

$$P(k|\mu,T) = \binom{T}{k} w_\mu^k (1-w_\mu)^{T-k} \approx \frac{(Tw_\mu)^k e^{-Tw_\mu}}{k!}, \tag{3}$$

where $w_k \equiv w_k(\infty)$, which can be approximated by the Poisson distribution, as in the rightmost term.

The total in-degree distribution after a time T, $P(k|T)$, is then given by

$$P(k|T) = \frac{1}{N} \sum_\mu P(k|\mu,T). \tag{4}$$

Now since a vertex μ is labeled uniquely by its hidden variable h_μ, we must have then that $w_\mu \equiv w(h_\mu)$. Thus, $w(h)$ can be obtained by rewriting Eq. (1),

$$w(h) = N \int_h r(h_\mu, h) w(h_\mu) \rho(h_\mu) dh_\mu, \tag{5}$$

assuming that h is a continuous variable (the last expression would just be a sum if it were discrete). Solving this integral equation for $w(h)$, it is possible then to obtain the degree distribution through Eq. (4),

$$P(k,T) = \int_h \frac{(Tw(h))^k e^{-Tw(h)}}{k!} \rho(h) dh. \tag{6}$$

1. In-degree correlation

It is also possible to calculate the degree correlation of this graph. The probability of one vertex μ, with in-degree k, connecting to another vertex of degree k' is given by

$$P(k'|k,\mu,T) = \frac{P(k|\mu,T)}{NP(k,T)} \sum_\nu P(\mu \to \nu) P(k'-1|\nu,T). \tag{7}$$

The total probability of one vertex with degree k connecting to one of degree k' is then simply

$$P(k'|k,T) = \sum_\mu P(k'|k,\mu,T), \tag{8}$$

and the average in-degree of the nearest out-neighbors is then just

$$\bar{k}_{NN}(k,T) = \sum_{k'} k' P(k'|k,T). \tag{9}$$

In terms of the hidden variables, substituting Eqs. (6) and (3) in (8) and calculating the sum in Eq. (9), we have then

$$\bar{k}_{NN}(k,T) = 1 + \frac{N}{P(k,T)} \int \int_h \frac{[Tw(h_\mu)]^k e^{-Tw(h_\mu)}}{k!} \times r(h_\mu, h_\nu) Tw(h_\nu) \rho(h_\mu) \rho(h_\nu) dh_\mu dh_\nu. \tag{10}$$

2. Attractor dynamics

We want to understand how correlations such as those seen in Figs. 6(b) and 6(c) and power-law distributions can arise from this type of network. For that we must define a

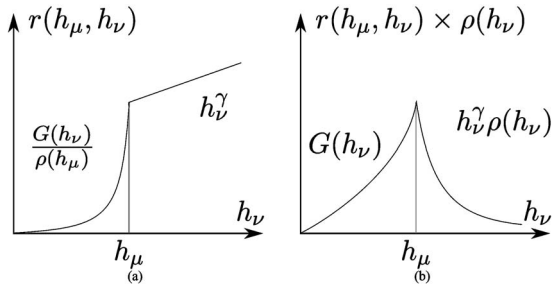

FIG. 10. (a) Connection probability [Eq. (11)] from a vertex μ to a vertex ν, and (b) connection probability from a vertex μ to any vertex with hidden variable h_ν.

suitable $r(h,h')$ and $\rho(h)$. It is clear that what uniquely defines the in-degree of some vertex is its hidden variable. Thus, for the in-degree correlation to be of the form $\bar{k}_{NN}(k) \sim k$ for large k, we must have that $\bar{h}'(h) \sim h$ for large h, where $\bar{h}'(h)$ is the average hidden variable of the out-neighbors of a vertex with hidden variable h. With this in mind, we define then the following general expression for the connection probability:

$$r(h_\mu, h_\nu) = F(h_\mu)\left(\frac{G(h_\nu)h_\mu^\gamma}{\rho(h_\nu)}[h_\nu < h_\mu] + \frac{G(h_\mu)h_\nu^\gamma}{\rho(h_\mu)}[h_\nu > h_\mu]\right) \tag{11}$$

where $G(h)$ is a function that dictates how fast the connection probability decays for $h_\nu < h_\mu$ (see Fig. 10), and the exponent γ defines the preference with which vertices with higher h are chosen. The function $F(h_\mu)$ is simply given by the normalization condition $\Sigma_\nu r(h_\mu, h_\nu) = 1$.

We considered a few shapes for $G(h)$ and $\rho(h)$ and calculated the degree distribution and degree correlation through Eqs. (6) and (10), always for $k \gg 1$. The results are summarized in Table I.

What we find is that the effect of adopting a connection probability like the one described by Eq. (11) is to generate an in-degree distribution corresponding to a stretched form of $\rho(h)$. If $G(h)$ is independent of h, and the trapping in the region of similar h is the weakest, we have the following possibilities. If $\rho(h)$ is a power law with exponent β, then $P(k)$ will also be a power law with exponent in the region $[1, \beta]$, approaching 1 if γ is large. When $\rho(h)$ is an exponential distribution, the resulting in-degree distribution will be a stretched exponential as indicated in Table I, which will also resemble a power law if γ is relatively large. Now, considering a stronger trapping effect with $G(h)$ increasing exponentially, we have that an exponential $\rho(h)$, with decay parameter β, is enough to create a power-law distribution of in-degrees, with exponents in the interval $[1, \beta]$, approaching 1 with faster $G(h)$. This means that it is not necessary to assume an intrinsic scale invariance, represented by a power law in $\rho(h)$, for the existence of a power law in $P(k)$. Furthermore, the asymptotic in-degree distribution in this case does not depend on γ, being totally dominated by the trapping behavior, and not by the preference of connection.

TABLE I. Different asymptotic shapes for $\bar{k}_{NN}(k)$ and $P(k)$ for different shapes of $G(h)$ and $\rho(h)$, for $k \gg 1$.

$\rho(h)$	$G(h)$	$\bar{k}_{NN}(k)$	$P(k)$
$\frac{h^{-\beta}}{\beta - 1}$	1	$\sim k$	$\sim k^{-(\beta+\gamma)/(\gamma+1)}$
$\beta e^{-\beta h}$	1	$\sim k$	$\sim k^{-\gamma/(\gamma+1)} e^{-Ck^{1/(\gamma+1)}}$
$\beta e^{-\beta h}$	$e^{\xi h}$	$\sim k$	$\sim k^{-(\beta+\xi)/\xi}$

The process described above shows a variety of ways in which graphs with in-degree distributions resembling power laws and linear in-degree correlation can be created. Looking at only these properties, it is not possible to know which one of the possibilities (if any) is more likely to describe the epicenter network. Moreover, the process above would not account for the strong synchronization observed in Figs. 8 and 9. After all, the sequences of epicenters are probably not simple Markovian processes. However, the above model, as a first approximation, serves the purpose of illustrating how such correlations and in-degree distribution can occur, and presents a general analytical framework for further modeling.

VI. CONCLUSIONS

We have shown that the epicenters in the OFC model occur predominantly near the boundary of the lattice, but this preference does not seem to scale with system size. This border affinity depends on the dissipation parameter α, being less for smaller values of α. It is also dependent on the earthquake size, with epicenters of larger earthquakes having a border effect which decays more slowly toward the bulk. We have also studied the network of consecutive epicenters, and found that it is sharply different in the two regimes of the model. In the conservative regime it is rather featureless, with uncorrelated in-degree statistics and Poisson in-degree distribution. However, in the nonconservative regime, it has an unusual linear degree correlation among vertices of high degree, and a broad distribution of in-degrees resembling a power law, but only when the smaller earthquakes are not considered. The in-degree distribution and correlation in this regime are similar to what was found very recently for real earthquakes [16,17]. Furthermore, we noticed that the high correlation of in-degrees is due to an attractor dynamics where the occurrence of epicenters tends to synchronize, with the same sequence of epicenters occurring continuously. This synchronization is broken by large earthquakes, which spread the epicenters over a larger portion of the lattice, thus populating the graph with vertices of smaller in-degree. Interestingly, the effects of the large events on the topology of the epicenter network are noticeable before the actual main event, and seem to be related to the series of increasingly larger foreshocks that precede it. Since the prediction of the OFC model that there would be an in-degree correlation in the epicenter graph corresponds to what has been recently found for real earthquakes [17], further detailed analysis of this behavior may prove useful for the prediction of large

earthquakes. Lastly, we described a general analytical network model based on a Markovian process and hidden variables, which is able to reproduce the most general aspects of the epicenter network, when a suitable attractor dynamics is specified. There are several aspects of the dynamics of epicenters that remain uncovered. It would be of special interest to look at other topological properties of the epicenter graph, such as the dependence of the clustering coefficient on in-degree, and the existence of community structure [25,26]. Furthermore, it would also be useful to compare in detail some of the results here obtained, such as the dynamics responsible for the in-degree correlation and the epicenter synchronization, with the epicenter network of real earthquakes.

ACKNOWLEDGMENT

This work was supported by Fundação de Amparo à Pesquisa do Estado de São Paulo (FAPESP), Process No. 03/03429-6.

[1] P. Bak, C. Tang, and K. Wiesenfeld, Phys. Rev. Lett. **59**, 381 (1987).
[2] B. Drossel and F. Schwabl, Phys. Rev. Lett. **69**, 1629 (1992).
[3] Z. Olami, Hans Jacob S. Feder, and K. Christensen, Phys. Rev. Lett. **68**, 1244 (1992).
[4] S. Lise and M. Paczuski, Phys. Rev. E **64**, 046111 (2001).
[5] S. Lise and M. Paczuski, Phys. Rev. E **63**, 036111 (2001).
[6] J. X. de Carvalho and C. P. C. Prado, Phys. Rev. Lett. **84**, 4006 (2000).
[7] B. Gutenberg and C. F. Richter, Ann. Geofis. **9**, 1 (1956).
[8] F. Omori, J. Coll. Sci., Imp. Univ. Tokyo **7**, 111 (1894).
[9] S. Hergarten and H. J. Neugebauer, Phys. Rev. Lett. **88**, 238501 (2002).
[10] T. P. Peixoto and C. P. C. Prado, Phys. Rev. E **69**, 025101(R) (2004).
[11] T. P. Peixoto and C. P. C. Prado, Physica A **342**, 171 (2004).
[12] A. A. Middleton and C. Tang, Phys. Rev. Lett. **74**, 742 (1995).
[13] M. E. J. Newman, SIAM Rev. **45**, 167 (2002).
[14] D. J. de S. Price, J. Am. Soc. Inf. Sci. **27**, 292 (1976).
[15] A.-L. Barabási and R. Albert, Science **286**, 506 (1999).
[16] S. Abe and N. Suzuki, Europhys. Lett. **65**, 581 (2004).
[17] S. Abe and N. Suzuki, e-print cond-mat/0602076.
[18] R. Burridge and L. Knopoff, Bull. Seismol. Soc. Am. **57**, 341 (1967).
[19] P. Grassberger, Phys. Rev. E **49**, 2436 (1994).
[20] B. Drossel, Phys. Rev. Lett. **89**, 238701 (2002).
[21] P. Erdös and A. Rényi, Publ. Math. (Debrecen) **6**, 290 (1959).
[22] R. Pastor-Satorras, A. Vázquez, and A. Vespignani, Phys. Rev. Lett. **87**, 258701 (2001).
[23] A. Helmstetter, S. Hergarten, and D. Sornette, Phys. Rev. E **70**, 046120 (2004).
[24] M. Boguñá and R. Pastor-Satorras, Phys. Rev. E **68**, 036112 (2003).
[25] M. E. J. Newman and M. Girvan, Phys. Rev. E **69**, 026113 (2004).
[26] S. Muff, F. Rao, and A. Caflisch, Phys. Rev. E **72**, 056107 (2005).